Appl Phys B
DOI 10.1007/s00340-012-4888-x

Applied Physics B
Lasers and Optics

An effective TDLS setup using homemade driving modules for evaluation of pulsed QCL

Y.G. Zhang · Y. Gu · Y.Y. Li · A.Z. Li · C. Li · Y.Y. Cao · L. Zhou

Received: 26 August 2011 / Revised version: 22 November 2011

Abstract Integrated, compact, and economical pulse driving and TE control modules for pulsed quantum cascade lasers (QCL) have been developed. Based on those modules, an effective tunable diode laser spectroscopy (TDLS) setup has been constructed for the evaluation of pulsed QCL and demonstration of TDLS concepts. Connecting our mid-infrared QCL module to the driving module using cable of 10 Ω characteristic impedance results in down chirp light pulses suitable for intrapulse scheme of TDLS; a usable down chirp of about 0.78 cm^{-1} is achieved for current pulse with 240-ns pulse width. Connecting the QCL module to the driving module using stripline of characteristic impedance <1 Ω results in narrow Gaussian-like light pulses that are suitable for interpulse scheme of TDLS; the light pulse width of 15 ns is achieved. The absorption features of N_2O at 1289.86 cm^{-1} have been measured using a homemade distributed feedback QCL around about 7.75 μm adopting intrapulse scheme; the measurement limit below 1 ppmv is achieved with a 10-m white cell.

Y.G. Zhang (✉) · Y. Gu · Y.Y. Li · A.Z. Li · C. Li · Y.Y. Cao · L. Zhou
State Key Laboratory of Functional Materials for Informatics, Shanghai Institute of Microsystem and Information Technology, Chinese Academy of Sciences, 865 Chang Ning Rd., 200050 Shanghai, China
e-mail: ygzhang@mail.sim.ac.cn
Fax: +8-621-52419931

C. Li · Y.Y. Cao · L. Zhou
Graduate School of the Chinese Academy of Sciences, Beijing 100049, China

1 Introduction

Tunable diode laser spectroscopy (TDLS) using quantum cascade lasers (QCLs) is becoming popular in recent years [1, 2]. Among various TDLS applications, the operation of pulsed QCLs at or above room temperature is still a meritorious option from synthetical point of view. In pulsed operation, the average power density on the QCL chip is quite low comparing to those of continuous-wave (CW) operation; also, in this case the thermal electric (TE) cooler is not used for removing mass heat energy but rather for stabilizing the operating temperature mainly, and therefore the power consumption of the system is much lower. Besides, the fabrication requirements for pulsed QCLs are not so strict comparing to those of CW QCLs and thus are beneficial to reduce the high price and encourage volume application. Different from near infrared communication band, where very mature techniques have existed already, and productive laser diode modules and driving integrated circuits (ICs) and modules are easily available, from the user's point of view, some blocks still exist in the utilization of QCLs in TDLS system. First, QCL is an unipolar device with much higher driving current and voltage than those of conventional bipolar diode laser, so the pulse driving technique suitable for bipolar diode laser may not be adopted directly; second, different types of QCL quantum engineering design, chip structure, package type, and so on result in quite different characteristics of the devices, and therefore more details accompanying each device are expected for the users. Furthermore, in the development of QCLs the variability of laser performance in a much wider range might be encountered. When newly developed QCLs being tested, the original equipment manufacturer (OEM) modules may not be appropriate, in this case homemade modules could be useful. In this paper, the development of integrated compact pulsed QCL driver

Published online: 07 February 2012

and TE controller with rich practical utilities has been introduced, and their applicability has been demonstrated in detail. Based on the homemade modules, a simple but effective TDLS setup with stable and maneuverable features has been constructed for the evaluation of different QCL chips and modules, and demonstration of TDLS concepts.

2 Homemade pulse driving and temperature control modules

Comparing with conventional bipolar diode lasers for communication etc., the operation of unipolar QCLs still needs some particular attentions. First, the operation current and voltage of QCL, as a rule of thumb, are on the 1 A/10 V level, which both are almost an order of magnitude higher than those of bipolar diode laser, and therefore special driving schemes should be adopted especially in pulse operation case; Second, different from bipolar laser where charge storage or capacitive component should be taken into account, inherently the unipolar QCL itself could be known as a "resistive" load, but in a certain case parasitic reactive components from the bonding, wiring, packaging, and connecting still play an important rule for pulse operation; Third, normally the equivalent on-state dynamic load resistance $\mathrm{d}V/\mathrm{d}I$ of the QCL is in a "medium" range of about 2–20 Ω, and most possibly 5–10 Ω. This resistance may be higher than those of bipolar diode lasers with even lower on-state dynamic resistance, say <2 Ω (may also reach ~ 10 Ω for devices with very small area), but still lower than the most popular system impedance of 50 Ω; therefore special care is needed for the impedance matching of the load to the driver. Furthermore, the on-state resistance of QCL contains nonohmic component inherently and therefore shows more notable nonlinear features than those of bipolar diode lasers. This means that the on-state dynamic resistances of QCLs are not fixed and the difference between off-state and on-state resistances is also quite large, which further increases the difficulties in the modeling and matching. Besides, different from the bipolar laser with lower driving power, the driving efficiency of this higher driving power device is another trait of concern. In a conventional 50-Ω system, a simple way to match a load with impedance less than 50 Ω is to insert a resistor in series with the load to reach a total impedance of 50 Ω; however, in this case the driving ability of the pulse generator will be degraded, especially for the high-power and high-operation-voltage load such as QCL. For example, using a power generator with 50-V output, its current driving ability is limited to 1 A in a 50-Ω system; this driving ability is enough for most bipolar diode lasers but still insufficient for QCL [3]. Also, in this case most power is consumed at the series resistor; for driving a high-power device, this is an inapposite way especially in practical applications.

In a TDLS setup using pulsed QCL, the performances and parameters of the pulse driving and temperature control modules are the first thing to be considered. From practical and mass application points of view, the simplicity and cost are important traits of concern, and therefore the modules should have no excrescent but all necessary functions; the parameters should cover a not excessive but needful range. Notice that the parameters are related to the key components employed in the module directly, and therefore adopting suitable components is important. Some high-end components with exorbitant performance are available, whereas the utilization of conventional components with lower but sufficient performance is a rational choice beneficial to the attainability, cost, and simplicity of the modules.

There are normally two schemes for making use of pulsed QCL into TDLS systems: intrapulse or interpulse [4]. For intrapulse scheme, normally "wider" current pulses with pulse width of hundreds of ns to a few μs with minimal transient are needed, whereas for inter-pulse scheme, shorter current pulses with pulse width below a few tens of ns are preferable. Notice that QCL is a current-driven device with certain threshold. If the threshold current is half of the peak operation current, using triangle or Gaussian-like current pulse, the light pulse width could also be half of the driving pulse width. Therefore, in certain conditions, using a 40-ns current pulse to generate a 20-ns light pulse is possible. In TDLS application the repeat frequencies of the current pulses are lower with respect to those of communication applications, and therefore the coverage of a few to tens of kHz is almost enough. For both intrapulse and interpulse schemes, normally distributed feedback (DFB) type of QCLs is used, and their threshold and operation currents are slightly higher than those of Fabry–Perot (FP) type due to the introduction of gratings. At early stage the threshold and operation currents of DFB-QCLs are in the range of 5–10 A for RT-CW devices [5] and then decrease to the 1–2 A range [6, 7]. The situation of pulsed QCL is similar. Therefore, the current driving ability up to 3 A is now enough for most cases. For convenience, the integration of driving current control, current pulse waveform monitor, and trigger outputs should be preferable. In certain applications the add-on of a slow scan current to the driving pulse is necessary, so the current modulation input and modulation waveform monitor output are needed. For the TE temperature controller, as mentioned above, the heat capacity is not important for TDLS system using pulsed devices [8], whereas wavelength/temperature coefficient in the order of –0.1 $\mathrm{cm}^{-1}/\mathrm{K}$ is inherent for DFB-QCLs [9, 10], and therefore the overall temperature stability of at least 0.05 K should be guaranteed. The temperature setting and reading functions of the module are needed in practice, but other functions seem superfluous.

Based on the above considerations, homemade integrated compact pulse driving module and TE temperature control module were developed. The pulse driving module was mainly composed of a transistor–transistor–logic (TTL) pulse generator, a voltage level shifter, and a vertical metal-oxide-semiconductor field-effect-transistor (MOSFET) current switch. The pulse generator using a conventional bipolar IC-produced pulses of width and frequency independently adjustable in TTL level. This small low-end IC could produce pulses with width down to <40 ns and rise/fall time of about 5 ns, which just fitted our needs. To increase the driving ability and as an isolator, a 50-Ω line driver IC composed of four nor-gates was followed, in which two gates in series were used to drive the voltage level shifter, and the others were used to output the trigger pulses. A MOSFET switch was used to output high-current pulse, so its performances were critical. In this driver an enhancement-mode (normally-off) vertical MOSFET was used. For the MOSFET, current handling ability, on-state resistance, transient time, and input capacitance are the key parameters. For example, high-end MOS transistors with a handling ability of tens of amperes for pulse current, <0.2 Ω on-state resistance, and <5 ns transient time could be available, but accompanying a higher input capacitance on the order of 1000 pF; therefore to drive this power MOS transistors, a specific CMOS driving module with high driving ability should be adopted. This combination seems prodigal and costly; thereby a trade-off should be taken. In our module an economical MOSFET in a small TO-243 package with 1.5-A continuous or 8-A pulsed current ability, 0.3-Ω on-state resistance, and ∼10-ns transient time is adopted, and its input capacitance decreased to about 200 pF, so conventional bipolar transistors were sufficient to drive it. In the pulse operation with low duty cycle, the average power on the MOSFET is lower, so for this device, only a small heat sink was used. For this enhancement-mode MOSFET, to get lower on-state resistance and faster transient time, about 10-V driving voltage should be needed normally; therefore a voltage level shifter composed of conventional bipolar transistors was inserted between the TTL pulse generator and MOSFET current switch. To monitor the real pulse current waveform using an external oscilloscope, a calibrated ring coil as current probe with 1-V/A output on 50-Ω loads was integrated into the module; an adjustable DC power source with a digital voltage meter (DVM) to monitor the output voltage was used to control the driving current.

For temperature controller with stability better than 0.05 K, even some multifunctional but costly commercial instruments could be utilized; a customized module should be more economical and easier to operate. In our homemade temperature control module a small commercial TE control board with moderate features was chosen to integrate with a power source as well as a DVM for external temperature setting and reading. This control board with >2 A current ability is sufficient for pulsed QCL operated at or above RT. The temperature sensor for our QCL module is a 10-KΩ thermistor, and based on this sensor, the measured overall temperature stability with the QCL module was better than 0.01 K.

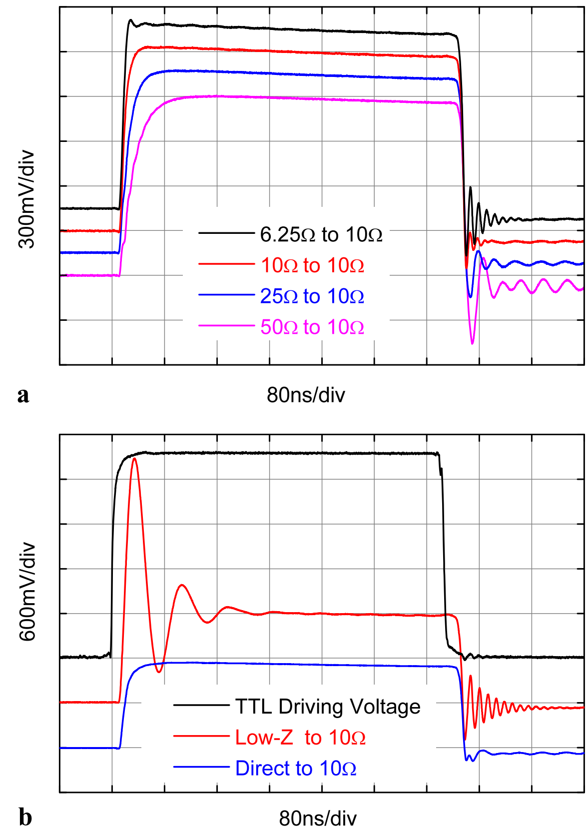

Fig. 1 Current waveforms of driving a 10-Ω resistive load using 500-ns-wide pulses at different matching conditions, the up trace in (**b**) is TTL driving voltage waveform

Some experiments were designed to evaluate the abilities of the modules. First of all, resistive loads were used to evaluate the driving ability of the pulse module. In the experiments different types of connections between the driver and resistive load were used to demonstrate matching conditions. The connections include cables with different characteristic impedance from 50 Ω to 6.25 Ω, stripline with metal width of 12 mm and characteristic impedance of <1 Ω (denoted as low-Z hereafter) and directly connecting the load to the driver (denoted as direct hereafter). Two load resistances of 10 Ω and 2 Ω were used to simulate the conditions of concern; the resistive load was composed of five 3216-size surface mount resistors in parallel to minimize the parasitic reactive components.

Figure 1 shows the driving of a 10-Ω load using 500-ns "wide" pulse at different matching conditions. From Fig. 1(b) it could be seen that the TTL driving pulse is quite good with neglectable ringing at falling edge, the transient time (20–80%) is about 5 ns. The direct driving of the 10-Ω load shows favorable fidelity, the rise time increases to about 10 ns, and a minor ringing appears at falling edge. From

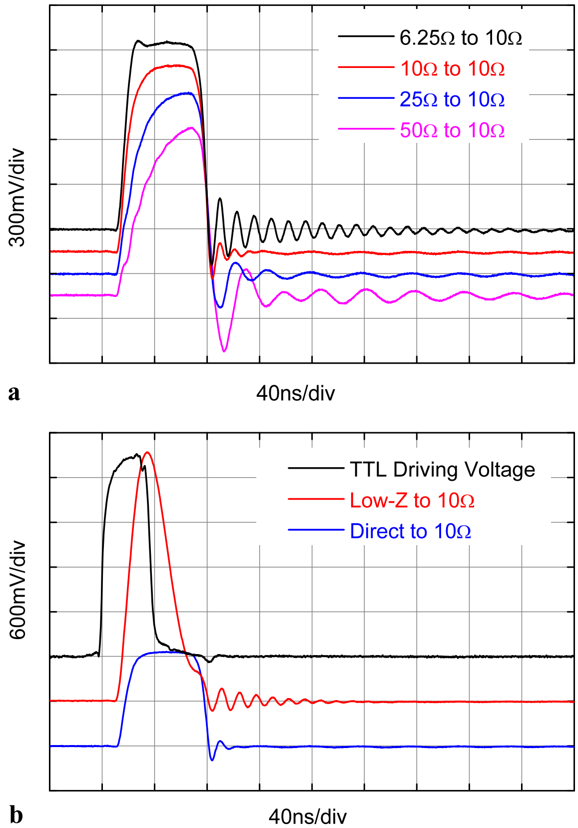

Fig. 2 Current waveforms of driving a 10-Ω resistive load using <40 ns narrow pulses at different matching conditions; the up trace in (**b**) is TTL driving voltage waveform

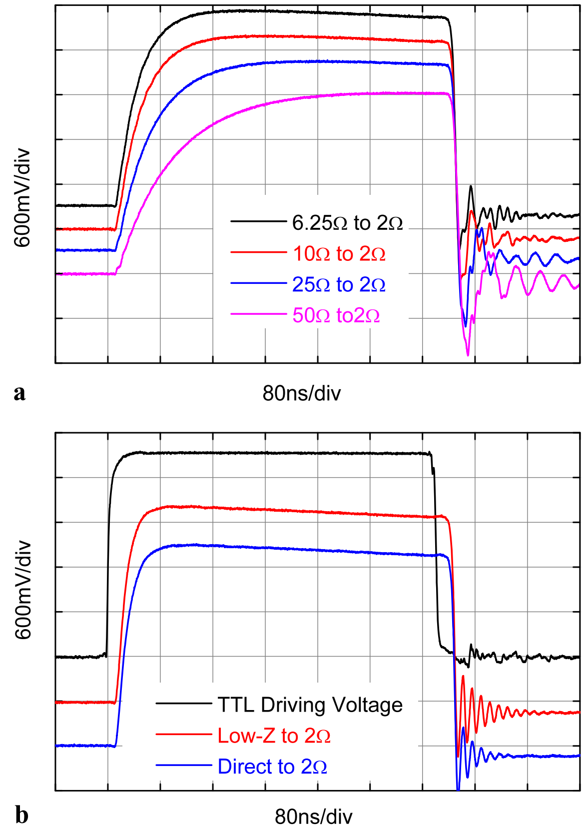

Fig. 3 Current waveforms of driving a 2-Ω resistive load using 500-ns-wide pulses at different matching conditions; the up trace in (**b**) is TTL driving voltage waveform

Fig. 1(a) it can be seen that using a 10-Ω cable matched to the load showed the best current waveform with minimal ringing at the falling edge and that the rise time keeps at about 10 ns without overshooting. However, the cables with higher or lower impedances aroused slowdown or minor overshoot at the rising edge, and obvious ringing at the falling edge. Notice that the subthreshold current ringing at the falling edge had no effects on the light output despite of negligible heating, also in most TDLS applications quite low duty cycle of the pulse was used, and therefore the ringing at falling edge was not important. For a 50-Ω cable, the rise time was slowed down to about 30 ns. At even lower impedance of low-Z stripline as shown in Fig. 1(b), a dramatic overshoot accompanying ringing process extending to about 200 ns appeared at rising edge, and the ringing at falling edge became more obvious. The overshoot reached about 3 times of the stable value, prompting a resonate process of the parasitic parameters mainly from the stripline.

Figure 2 shows the driving of a 10-Ω load using <40 ns narrow pulse at different matching conditions. From Fig. 2(b) it could be seen that the TTL driving pulse was still moderate with neglectable ringing and that the transient time remained about 5 ns with 36-ns pulse width. The direct driving of the 10-Ω load still showed favorable fidelity, but the current pulse width broadened to 58 ns with minor ringing at falling edge. From Fig. 2(a) it can be seen that, using a −10 Ω cable matched to the load also showed the best current waveform with minimal ringing at the falling edge, the rise time kept at about 10 ns without overshooting, and the current pulse width was 60 ns. The cables with higher or lower impedances also aroused slowdown or minor overshoot at the rising edge, and obvious ringing appeared at falling edge. For a 50-Ω cable, the rise time was still slowed down to about 30 ns. At even lower impedance of low-Z stripline as shown in Fig. 2(b), the resonance process resulted in a Gaussian-like high-current pulse about 3 times of the other impedance accompanying a small ringing tail, and the current pulse width was about 33 ns. Recall that although in this case the fidelity of the pulse is poor, this narrow current pulse with higher amplitude could be utilized to generate short light pulse.

The situation to drive a 2-Ω load became different. Figure 3 shows the driving of a 2-Ω load using 500-ns "wide" pulse at different matching conditions. From Fig. 3 it can be seen that cable impedance higher than the load resulted in an unacceptable slowdown at the rise edge, but low-impedance stripline showed favorable matching to the load with rise time about 20 ns similar to the direct connection. At the con-

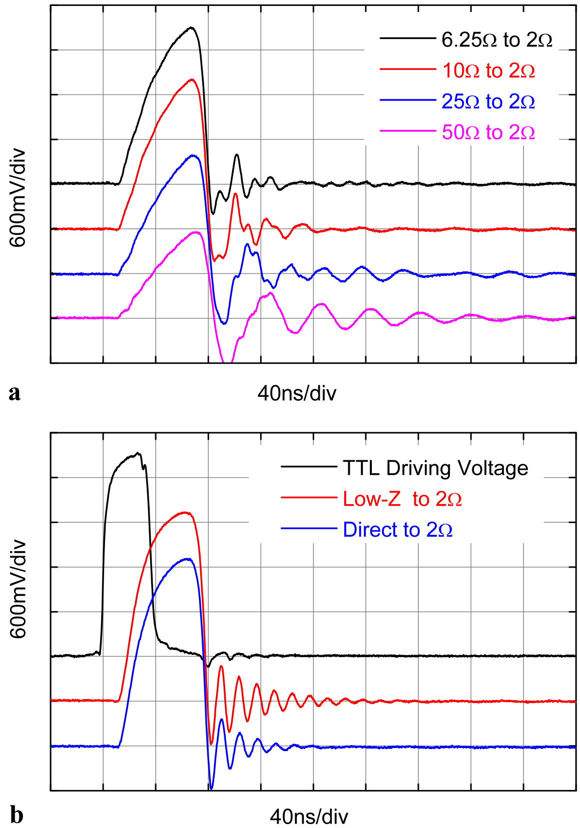

Fig. 4 Current waveforms of driving a 10-Ω resistive load using <40 ns narrow pulses at different matching conditions; the up trace in (**b**) is TTL driving voltage waveform

dition with <40 ns narrow pulse driving as shown in Fig. 4, analogous phenomena existed. The driving of 2-Ω load using low-impedance stripline resulted in a slightly broadened current pulse with 52-ns pulse width, but cable impedance higher than load all resulted in unacceptable waveforms. Consequently, to drive a low resistance load down to 2 Ω, the cable impedance should be comparable, so in this case the low-impedance stripline was a good choice.

From the above results it could be deduced that the output impedance of this driving module was quite low (<2 Ω), which was benefitted from the low on-state resistance of the MOSFET. To get favorable pulse current waveforms and therefore desired light pulses, the matching of pulse generator to the load played an important role, so suitable cables should be adopted. Different from conventional 50-Ω systems, where all connections were attributed to 50-Ω impedances, in most cases cable impedance close to the load dynamic impedance was advisable for this type of driving scheme. However, in certain case, the resonance feature in the connection could also be utilized to generate shorter and higher current pulses. The light output was detected using a Vigo MCZT detector (PVI-2TE-10.6/VPDC250I) with an integrated preamplifier (DC coupled, 250-MHz bandwidth). This PD/amplifier combination resulted in ≤3 ns time response. All waveforms were recorded using a digital oscilloscope (Tektronics TDS3054, 5GS/s, 500-MHz bandwidth) of <1 ns time response. The overall time resolution of the measuring system was below 3 ns, and therefore the measured transient time of about 5 ns denoted the time response of this QCL/driver combination. The main parameters of the modules are listed in Table 1.

Table 1 Main parameters of the homemade pulse driving and TE temperature control modules

Pulse driving module	
Driving current	Up to 3 A (with 10 turn trimpot fine adj.)
Driving voltage	Up to 20 V (with DC DVM monitor)
Light pulse width	15–2500 ns (in N-M-W with fine adj.)
Light pulse frequency	1–100 KHz (in L-M-H with fine adj.)
Output connector	D-9pin (F) with on/off and indicator
Output current monitor	1 V/A real waveform into 50 Ω (SMA-F)
Trig. pulse output	TTL into 50 Ω (SMA-F)
Pulse rise/fall time	≤10 ns
LF modulation input	≤5 V (SMA-F)
LF modulation monitor	50 mA/V (SMA-F)
AC power	90–264 V fused, <10 W
Size	135 mm (W) × 72 mm (H) × 104 mm (D)
Weight	720 g
TE temperature control module	
Output current	±2 A
Compliance voltage	9 V
Temperature range	10–50°C
Temperature stability	<0.01°C
T setpoint accuracy	<0.01°C (with 10 turn trimpot fine adj.)
T reading accuracy	<0.05°C (with DVM monitor)
Output connector	D-9pin (M) with on/off and indicator
AC power	90–264 V fused, <20 W
Size	135 mm (W) × 55 mm (H) × 220 mm (D)
Weight	1000 g

3 QCL evaluation, TDLS setup and demonstration

Figure 5 shows the current and light output waveforms of our QCL module by using homemade pulse driving module. The QCL chip in the module was a gas source molecular beam epitaxy (GSMBE) grown DFB type with deep top gratings [10], which was mounted on a C-type submount, packaged into a TO-3 type package with a semi-insulating GaAs window and installed into an ILX lightwave LDM-4412 laser diode mount. The laser diode mount was modified for mid-infrared application using an adjustable ZnSe collimating lens, the mounting plate was changed to

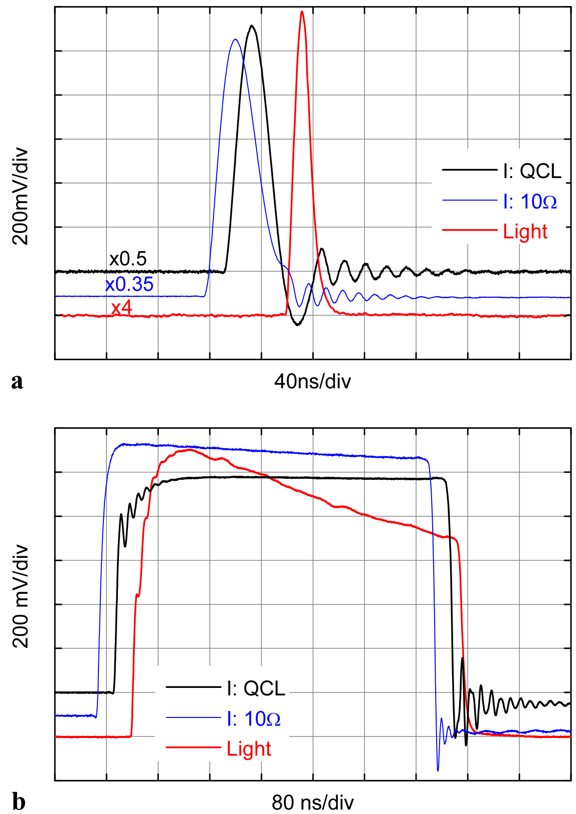

Fig. 5 Current and light waveforms of driving a homemade QCL module. (**a**): Using <40 ns narrow pulses with a low-Z stripline; (**b**): Using 500-ns pulses with a 10-Ω cable. For comparison, the current waveforms of driving a 10-Ω load were also plotted

fit TO-3 package, and the internal connection was modified for ∼12.5 Ω impedance. From Fig. 5(a) it could be seen that, beginning from 36-ns TTL pulses, operating the QCL adopting a low-Z stripline connecting to this driver resulted in Gaussian-like current pulses of width of 27 ns and peak >2 A. Due to about 1-A threshold current of this QCL, Gaussian-like light pulses of width about 15 ns were achieved, and those narrow light pulses were suitable for interpulse applications in TDLS. For 500-ns TTL pulses, operating the QCL adopting a 12.5-Ω cable connection to this driver resulted in different current and light waveforms as shown in Fig. 5(b). In this case the cable impedance was quite close to but slightly higher than the dynamic resistance of this QCL; the difference between the width of current and light was <20 ns, and no overshooting appeared at the light waveform. A decrease of the light amplitude with the time because of the heating effect of the "wide" pulse driving could be seen, and the usable down chirp range during this pulse was >400 ns, which was quite suitable for intrapulse applications in TDLS. For comparison, the current waveforms of driving a 10-Ω resistor load using 10-Ω cable or low-Z stripline (similar to the case in Fig. 1 or Fig. 2) were also plotted in Fig. 5. It could be seen that the waveform to driving this QCL is comparable to a ∼10-Ω resistor load, but effects of parasitic parameters still could be seen from the transient edges. QCL as an unipolar device could be seen as a resistive dominating load, and thus for a low-impedance driver, using a driving cable with impedance comparable to the dynamic resistance of the QCL chip is advisable, whereas the reactance parts of the QCL module mainly caused by packaging (wire bonding) and wiring should be minimized.

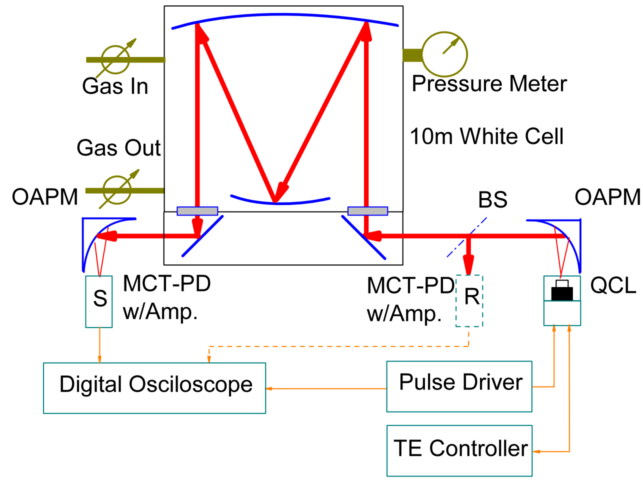

Fig. 6 Schematic configuration of the TDLS setup

Based on developed homemade modules, an effective TDLS setup mounted on a 30 × 60 cm optical breadboard using only a few parts was constructed; the schematic of this setup is shown in Fig. 6. The main purpose of this setup was the evaluation of different pulsed QCL chips and modules to meet the wide range of requirements and demonstrate basic TDLS schemes using those QCLs. In this setup the pulse module was used to driving the QCL under test. The light from the QCL was collected and collimated toward the gas cell using a 90° off-axis parabolic mirror (OAPM) of 1 inch in diameter. A commercial 10-m white cell for Fourier transformed infrared (FTIR) spectrometer originally was used in the system; the wide and parallel beam features of this gas cell made the system quite stable and easy to operate. The light out-off the gas cell was focused using another OAPM to a Vigo MCZT detector (model PVI-2TE-10.6/VPDC250I) to form absorption signal. To get a reference light, a MIR beam splitter was used at the front side of the gas cell, and another Vigo MCZT detector (the same model) was used to form the reference.

In this setup various characteristics of the QCL chips and modules related to TDLS applications, including suitable driving current and related DC voltage, favorable pulse parameters and impedance matching conditions, down chirp rate, modulation parameters and related temperature parameters, have been evaluated in detail. Through the optimization of each parameter, TDLS concepts were demon-

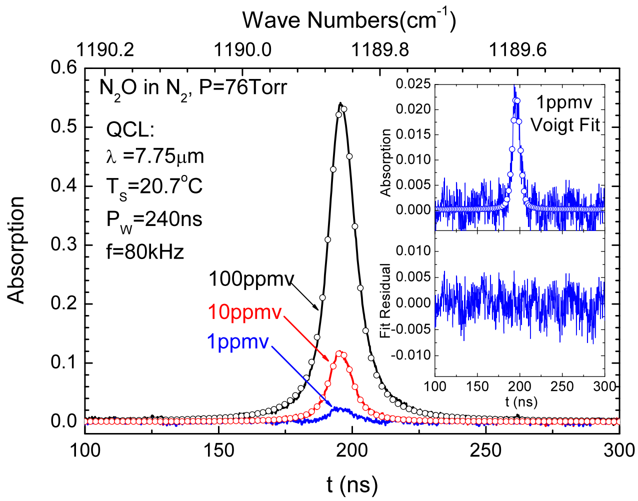

Fig. 7 Measured absorption features of N_2O line at 1289.86 cm^{-1} adopting a homemade DFB-QCL in intrapulse scheme, the N_2O is diluted using N_2 to 100, 10 and 1 ppmv. *Solid curves* show the ratio of signal to the reference, *open circles* show the Voigt fittings. The *inset* shows the zoom in of 1-ppmv curve, Voigt fit, and the residual

strated on this setup. Figure 7 shows a measured absorption features of N_2O line at 1289.86 cm^{-1}, with N_2O diluted using N_2. In this measurement the intrapulse scheme is adopted, a homemade DFB-QCL chip [10] with wavelength around 7.75 μm was used as a mid-infrared light source. This chip was mounted on ST submount, then installed into an Alpes LLH100 air-tightened laser housing without collimating lens, and a 10-Ω cable was used to connect the DFB-QCL module to the driving module. Current pulses of 240-ns pulse width and 80-kHz repeat frequency were used, resulting in >200 ns usable down chirp time. At higher concentration of 1000 ppmv, two weaker absorption lines at both sides could be clearly seen; according to HITRAN database, those lines could be assigned to 1290.119 cm^{-1} and 1289.643 cm^{-1} lines of N_2O. From this the chirp rate of the QCL has been determined to be −116.5 MHz/ns (−3.885E–3 cm^{-1}/ns) and keeps constant during the pulse, which is lower than some reported values [4, 11–13] because of the lower threshold current density of the QCL. The wave number scan range was about 0.78 cm^{-1}. In the measurements the heatsink temperature of QCL was stabilized at 20.7°C. For simplicity, in this intrapulse scheme demonstration only an oscilloscope (Tektronics TDS3054) was used to record signal and reference waveforms, and the TTL output from the pulse driving module was used to trigger the synchronization. The waveform calculation function of the oscilloscope could be used to ratio the signal with the reference to form absorption waveform, whereas in this case a 50-Ω cable with length equivalent to the path length of the gas cell should be used to delay the reference signal.

Absorption full width at half maximum of 9.8 ns and 11.8 ns was observed for 10 ppmv and 100 ppmv of N_2O at 76 torr, respectively, confirming the self-broadening effect in this pressure and concentration range. The Voigt fits were also plotted in Fig. 7. The fits matched the measured absorption curves well: for 100 ppmv and 10 ppmv curves, the maximum fit residuals were below 2.4% and 10% respectively. At this pressure and concentration range the dominant source of line broadening is due to collisions of gas molecules, and therefore the lines are mainly of Lorentzian shape. From Voigt fits the Lorentzian width broadened from 7.25 ns to 9.24 ns for 10 ppmv and 100 ppmv in time domain, whereas the Gaussian width kept almost unchanged at about 5.6 ns. Notice that simulations based on HITRAN database resulted in much narrower line width of 506 MHz and 664 MHz for 10 ppmv and 100 ppmv of N_2O at 76 torr, respectively, and the Doppler line width is only ∼100 MHz, so the measured data in this setup are all limited by the chirp rate of the laser and the transient response of the system. The parameters extracted from the automatic Voigt fits are qualitative even if the line shape fits well. The inset in Fig. 7 showed the zoom in of 1 ppmv curve as well as Voigt fit and residual. At this concentration the maximum fit residual was about 20%, so for this setup, the N_2O measurement limit below 1 ppmv was evident.

4 Conclusions

In conclusion, through the analysis of characteristic features of the pulsed QCL and from effective and practical considerations, integrated compact and economical pulse driving and TE control modules were developed. Based on those modules, an effective TDLS setup was constructed for the evaluation of pulsed QCL and demonstration of TDLS concepts. Connecting the QCL to the driving module using low-Z stripline resulted in narrow Gaussian-like light pulses suitable for interpulse scheme of TDLS; the light pulses with pulse width of 15 ns was achieved. Connecting the QCL to the driving module using a 10-Ω cable resulted in down chirp light pulses suitable for intrapulse scheme of TDLS, and a down chirp of about 0.78 cm^{-1} was achieved for 240-ns current pulse. The absorption features of N_2O around 7.75 μm have been measured using a homemade DFB-QCL in intrapulse scheme; the measurement limit below 1 ppmv was achieved with a 10-m white cell.

Acknowledgements This work is financially supported by Knowledge Innovation Program of the Chinese Academy of Sciences under grant No. KJCX2-SW-W27 and National Basic Research Program of China under grant No. 2012CB619200.

References

1. F.K. Tittel, Y. Bakhirkin, A.A. Kosterev, G. Wysocki, Rev. Laser Eng. **34**, 275 (2006)

2. R.F. Curl, F. Capasso, C. Gmachl, A.A. Kosterev, B. McManus, R. Lewicki, M. Pusharsky, G. Wysocki, F.K. Tittel, Chem. Phys. Lett. **487**, 1 (2010)
3. Y.G. Zhang, K.J. Nan, A.Z. Li, Spectrochim. Acta Part A **58**, 2323 (2002)
4. J. Manne, W. Jäger, J. Tulip, Appl. Phys. B **97**, 334 (2009)
5. D. Hofstetter, M. Beck, T. Aellen, J. Faist, Appl. Phys. Lett. **78**, 398 (2001)
6. J.S. Yu, S. Slivken, S.R. Darvish, A. Evans, B. Gokden, M. Razeghi, Appl. Phys. Lett. **87**, 041104 (2005)
7. S.R. Darvish, W. Zhang, A. Evans, J.S. Yu, S. Slivken, M. Razeghi, Appl. Phys. Lett. **89**, 251119 (2006)
8. C. Zhu, Y.G. Zhang, A.Z. Li, Z.B. Tian, J. Appl. Phys. **100**, 053105 (2006)
9. Y.G. Zhang, G.Y. Xu, A.Z. Li, Y.Y. Li, Y. Gu, S. Liu, L. Wei, Chin. Phys. Lett. **23**, 1780 (2006)
10. G.Y. Xu, A.Z. Li, Y.Y. Li, L. Wei, Y.G. Zhang, C. Lin, H. Li, Appl. Phys. Lett. **89**, 161102 (2006)
11. M.T. McCulloch, E.I. Normand, N. Langford, G. Duxbury, J. Opt. Soc. Am. B **26**, 1761 (2003)
12. S. Welzel, G. Lombardi, P.B. Davies, R. Engeln, D.C. Schram, J. Röpcke, J. Appl. Phys. **104**, 093115 (2008)
13. J.A. Nwaboh, O. Werhahn, D. Schiel, Appl. Phys. B **103**, 947 (2011)